

Inverse magnetocaloric effect in sol–gel derived nanosized cobalt ferrite

E. Veena Gopalan · I.A. Al-Omari · D. Sakthi Kumar ·
Yasuhiko Yoshida · P.A. Joy · M.R. Anantharaman

Received: 23 September 2009 / Published online: 14 February 2010
© Springer-Verlag 2010

Abstract The magnetocaloric properties of cobalt ferrite nanoparticles were investigated to evaluate the potential of these materials as magnetic refrigerants. Nanosized cobalt ferrites were synthesized by the method of sol–gel combustion. The nanoparticles were found to be spherical with an average crystallite size of 14 nm. The magnetic entropy change (ΔS_m) calculated indirectly from magnetization isotherms in the temperature region 170–320 K was found to be negative, signifying an inverse magnetocaloric effect in the nanoparticles. The magnitudes of the ΔS_m values were found to be larger when compared to the reported values in the literature for the corresponding ferrite materials in the nanoregime.

1 Introduction

The magnetocaloric effect (MCE) is the heating produced in a magnetic material under an applied magnetic field and cooling when the applied magnetic field is removed [1, 2].

The magnetocaloric effect is being exploited not only for room-temperature refrigeration but also for a variety of other cooling applications ranging from production of low temperatures (millikelvin) to room-temperature refrigeration [3, 4]. The phenomenon of the magnetocaloric effect can also be perceived as a heat engine and hence assumes significance for heating applications, too [5]. Materials exhibiting large magnetocaloric effect near room temperature (250–300 K) are of particular interest because of energy savings and environmental concerns compared with the conventional gas-phase refrigeration [6]. Miniaturization of cooling devices has become a necessity considering the proliferation of micro- and nanoscale electromechanical systems (MEMS and NEMS) [7]. With the advent of nanoscience and nanotechnology, a horde of nanocrystalline materials is being investigated as potential refrigerants and among them Gd and Gd-based alloys lead the table of potential materials for refrigeration [8–10]. Other promising materials are lanthanum perovskite manganites, Heusler alloys, MnAs-based compounds, La(Fe,Si)₁₃-type alloys, etc. [11–13].

Though ferrites in principle are potential magnetic refrigerants, there was not much focus on these materials since room-temperature refrigeration demands materials with low Curie temperatures. This is because the operating temperature of a magnetic refrigerant must be near its Curie temperature where there is maximum ordering. The field under which maximum cooling is produced is also critical for applications, since ordinary electromagnets or permanent magnets can be employed for the production of magnetic cooling. Nanosized ferrites are seen as promising candidates for magnetic refrigeration and research activities on the magnetocaloric properties are on the rise [14]. When their size is reduced they become single domain accompanied by a reduction in T_c (Curie temperature) and at a certain critical size they become superparamagnetic or exhibit

E.V. Gopalan · M.R. Anantharaman (✉)
Department of Physics, Cochin University of Science and Technology, Cochin 682 022, Kerala, India
e-mail: mraiyer@gmail.com

I.A. Al-Omari
Department of Physics, College of Sciences, Sultan Qaboos University, PO Box 36, PC 123, Muscat, Oman

D.S. Kumar · Y. Yoshida
Bio-Nano Electronics Research Centre, Department of Applied Chemistry, Toyo University, Kawagoe, Saitama 350-8585, Japan

P.A. Joy
Physical Chemistry Division, National Chemical Laboratory, Pune 411 008, India

spin glass like behavior [15]. The suitability of such materials for magnetocaloric application then depends on their blocking temperature T_b or glass transition temperature T_g and the numerical values of the magnetocaloric effect, ΔS_m or ΔT_{ad} . Extensive investigations delving into the magnetocaloric properties of nanosized ferrites are ongoing and there are various reports on the magnetocaloric properties of manganese zinc ferrites and cobalt ferrites [14, 16].

Cobalt ferrite with its high coercivity, moderate magnetization and very high magnetocrystalline anisotropy is one of the technologically important ferrites. Cobalt ferrites, with particle size less than 10 nm, are of interest because they exhibit interesting magnetic and structural properties [17]. At sizes < 5 nm they are found to be exhibiting superparamagnetic properties [18]. Cobalt ferrite can be prepared in the nanoregime by cold precipitation techniques or sol-gel techniques. Cobalt ferrite, because of its large magnetocrystalline anisotropy, is expected to exhibit non-zero coercivity even at very small particle sizes of the order of 5 nm and is a promising candidate for many applications, namely magnetic data storage, magnetic drug targeting, biosensors, tumor treatment and magnetic refrigeration [19, 20].

Decreased particle size leads to decreased H_c (coercivity) and T_c , but an increased anisotropy at the nanodimensions results in increased T_b in cobalt ferrite nanoparticles. Hence, the blocking temperature T_b in cobalt ferrite nanoparticles can be suitably tuned to room temperature by exploiting the anisotropy factor. Since the blocking temperature corresponds to a magnetic transition, one can expect an enhanced entropy change around this ordering temperature. Also, the field required for an enhanced magnetic entropy change in the case of nanoparticles is relatively small. This would increase the efficiency of the refrigerator as well as reduce its size due to the reduction in cooling requirements. Thus, nanosized cobalt ferrite is of interest as far as its magnetocaloric properties are concerned. The ability to tailor the ordering temperature by tuning the size of the crystallite is an added advantage as far as the choice of the operating temperature of the refrigeration system is concerned.

The magnetocaloric effect can be observed either as an adiabatic temperature change ΔT_{ad} or as an isothermal entropy change ΔS_m . They can be derived from Maxwell's thermodynamic relations as [21]

$$\Delta S_m(T, H)_{\Delta H} = \int_{H_I}^{H_F} \frac{\partial M(T, H)}{\partial T} dH, \quad (1)$$

$$\Delta T_{ad}(T)_{\Delta H} = - \int_{H_I}^{H_F} \left(\frac{T}{C(T, H)} \right) \left(\frac{\partial M(T, H)}{\partial T} \right) dH. \quad (2)$$

The indirect technique of measuring the MCE from magnetization data involves the numerical integration of (1). This equation relates the entropy change to the application of an external magnetic field H , in terms of measurable

quantities M , T and H . If one measures the magnetization as a function of field at various temperatures, then ΔS_m can be approximated as follows [22]:

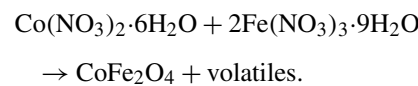
$$\Delta S_m \cong \frac{1}{\Delta T} \left[\int_0^H M(T + \Delta T, H) dH - \int_0^H M(T, H) dH \right]. \quad (3)$$

The above equation shows that the change in entropy of a system is equivalent to the area between the two magnetic isotherms divided by the temperature difference between the isotherms. This formulation is useful for graphical or numerical calculations of ΔS_m from the magnetization data. Thus, the magnetocaloric effect can be estimated without employing calorimetric techniques. The typical error involved in these measurements is found to be around 8% [23]. Here, ΔS_m values for cobalt ferrite nanoparticles that are reported result indirectly, with numerical methods applied to measured isothermal thermomagnetization curves.

2 Experimental

2.1 Synthesis

Fine particles of cobalt ferrite were synthesized by the sol-gel combustion method. For this, cobalt nitrate and ferric nitrate of AR grade chemical precursors were used with ethylene glycol as the solvent. Cobalt nitrate and ferric nitrate were dissolved in ethylene glycol in the molar ratio of 1:2 at 40°C to form the sol. This sol was then heated slowly to 60°C and the temperature was kept constant until a wet gel of the metal nitrates was obtained. The gel was then dried at 90°C. This resulted in the self ignition of the gel, producing a highly luminous and fluffy product which was ground to obtain fine powder. The combustion can be considered as a thermally induced redox reaction of the gel wherein ethylene glycol acts as a reducing agent. The nitrate ion acts as an oxidant. The nitrate ion provides an in situ oxidizing environment for the decomposition of the organic component. The chemical reaction leading to the formation of cobalt ferrite is as follows.



2.2 Structural and magnetic characterization

The samples were characterized by using an X-ray powder diffractometer (XRD, Rigaku Dmax-C) using Cu-K α radiation ($\lambda = 1.5405$ Å). The lattice parameter was calculated assuming cubic symmetry [24]. The average crystallite size was determined from the measured width of their

diffraction curves by using the Debye–Scherrer formula. The particle size of the sample was determined by subjecting the sample to transmission electron microscopy (TEM, Jeol JEM-2200 FS). High resolution transmission electron microscopy (HRTEM) images and energy dispersive X-ray spectra (EDS) were also obtained. A Thermo Electron Corporation, model IRIS Intrepid II XSP spectrometer was used for inductively coupled plasma (ICP) analysis measurement. Magnetic and MCE characterization were carried out using a vibrating sample magnetometer (VSM, DMS 1660, Oxford Instruments) with an external magnetic field varying from -13.5 to 13.5 kOe. The sweep rate of the field is slow enough to ensure that the isotherms are recorded in an isothermal process. In the present investigation, field cooling–zero field cooling (FC–ZFC) modes of the VSM were employed for the FC–ZFC measurements. In the ZFC mode, the sample was cooled in the absence of a field and the magnetization was measured during warming, by applying a nominal field of 500 Oe. In the FC mode, the sample was cooled in the presence of a field and the magnetization was measured during warming, under the field of 500 Oe.

3 Results and discussion

3.1 Structural and magnetic characterization

The XRD pattern (Fig. 1) indicates the formation of phase pure cobalt ferrite having a crystallite size of 13.8 nm. The lattice parameter ‘ a ’ for the sample was found to be 8.413 \AA . It should be noted that the lattice parameter of the bulk cobalt ferrite is 8.391 \AA (ICDD file no. 22-1086). The mean particle size of around 13 nm determined from TEM (Fig. 2) is in agreement with the crystallite size obtained using XRD.

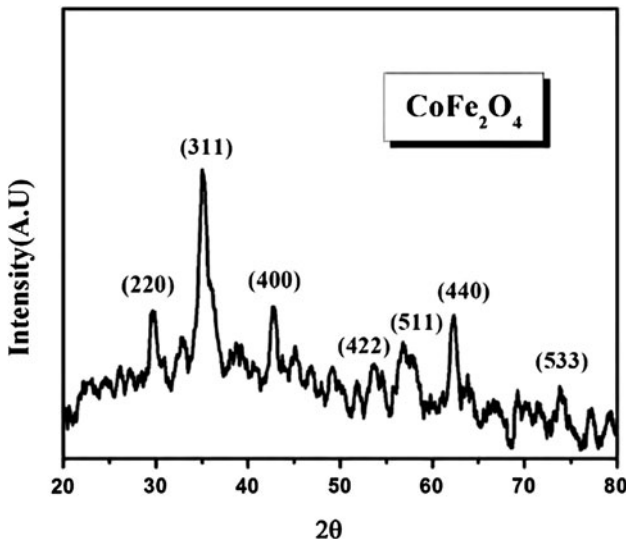


Fig. 1 XRD diffraction pattern of cobalt ferrite

The HRTEM images clearly depict the crystal planes corresponding to cobalt ferrite (Fig. 3). The EDS spectrum (Fig. 4) of the cobalt ferrite sample indicates that the Co:Fe ratio is 1:2 and hence the loss of ferric or cobalt ion is ruled out. The elemental ratio obtained from ICP measurements was also consistent with those obtained from EDS analysis.

The hysteresis loops for CoFe_2O_4 at two different temperatures (300 and 100 K) are depicted in Fig. 5. The hysteresis loop parameter M_s (saturation magnetization per unit mass) and H_c (coercivity) values for the sample were evaluated from the M – H curves as $48\text{ A m}^2/\text{kg}$ and $85987\text{ A m}^{-1}\text{ Oe}$ at 300 K. The samples do not exhibit any superparamagnetism at room temperature. The magnetization does not saturate even at the maximum applied magnetic field of 13.5 kOe. High magnetic crystalline anisotropy

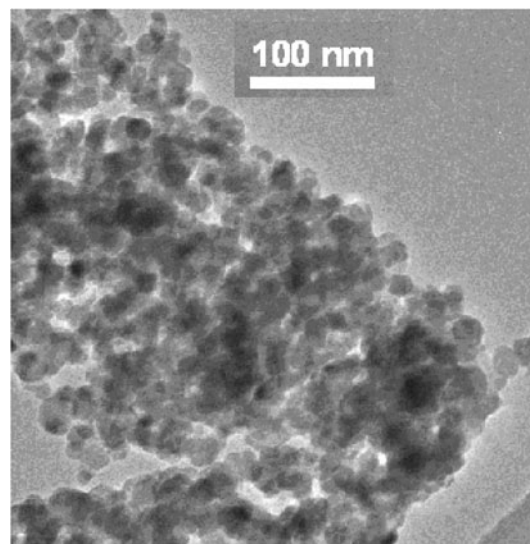


Fig. 2 TEM image of cobalt ferrite nanoparticles

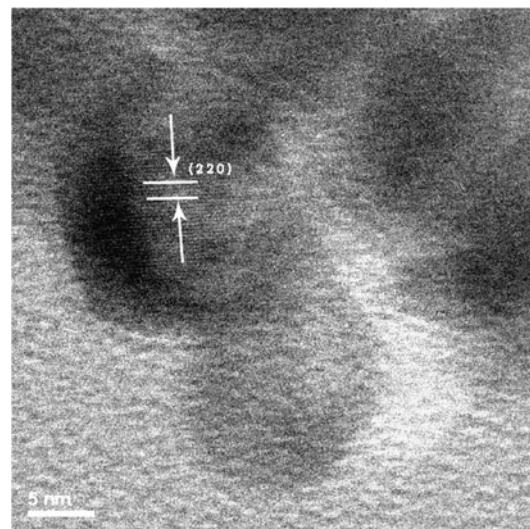


Fig. 3 HRTEM image of cobalt ferrite nanoparticles

Fig. 4 EDS pattern of cobalt ferrite

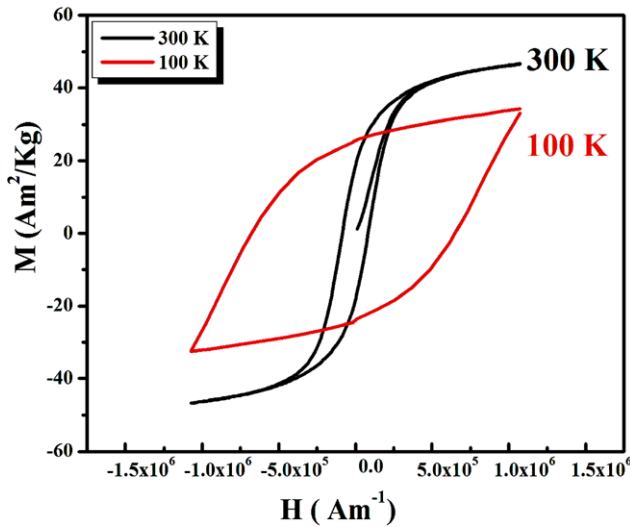
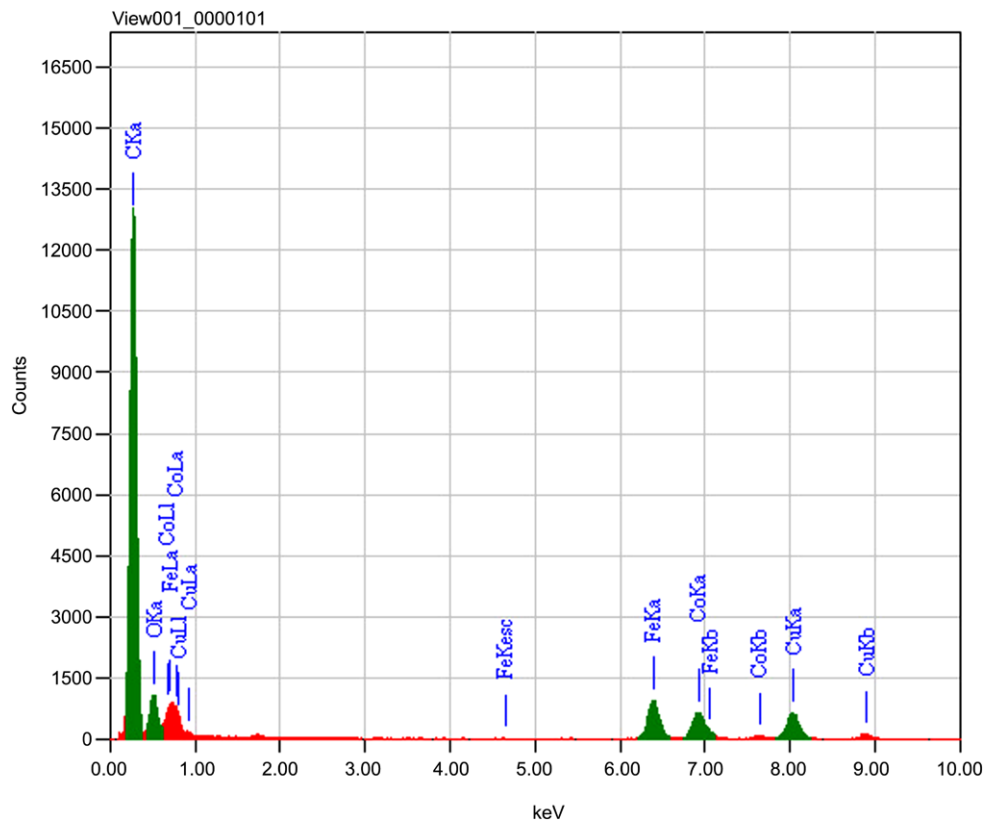


Fig. 5 Hysteresis curves at 300 and 100 K

associated with cobalt ferrite can be the cause of this type of behavior [25]. A much broader hysteresis curve is observed for the sample at 100 K, reflecting an immense increase in the coercivity at low temperature.

The ratio M_r/M_s (magnetic remanence/saturation magnetization) throws light on the exchange interactions and magnetocrystalline anisotropy associated with the ferrite nanoparticles [26]. According to the Stoner–Wohlfarth

model [27], theoretical value of M_r/M_s is 0.5 for non-interacting uniaxial single domain particles with the easy axis being randomly oriented. The M_r/M_s value observed is found to be 0.41 for the sample. Hence, these cobalt ferrite nanoparticles exhibit uniaxial anisotropy. There is an increase in M_r/M_s values measured at 100 K. This points towards the increase in magnetocrystalline anisotropy associated with decreased temperature. The maximum M_r/M_s value is found to be 0.66, indicating the enhanced contribution from cubic anisotropy (higher-order terms of magnetocrystalline anisotropy) at lower temperature. Hence, a large coercivity can be expected at lower temperature.

The magnetization value of the sample was found to be lower than that of its bulk counterpart. However, other factors like cation redistribution in the nanoregime, surface effects like spin-glass formation, finite size effects and presence of a dead layer, all can contribute to the reduction in magnetization. The reduction in magnetization can also be attributed to the presence of Co^{3+} ions and also a cation distribution with cobalt ions on the tetrahedral sites.

Zero field cooled experiments provide a means of investigating the effects of the various magnetic interactions. For the ZFC measurements, the sample was cooled from room temperature to 12 K without any external magnetic field and the magnetization was recorded while warming the sample in the applied field. Normally, the ZFC curve of nanoparticles is characterized by a cusp at a particular temperature

called the blocking temperature, T_b . Above T_b the particles are superparamagnetic with zero coercivity while a hysteresis loop appears below T_b . Field cooled measurements proceed in a similar manner to ZFC except that a constant external field is applied while cooling and heating. The net moment is usually measured while heating; however, the FC curve will diverge from the ZFC curve at a point near the blocking temperature. This divergence occurs because the spins from each particle will tend to align with the easy crystalline axis that is closest to the applied field direction and remain frozen in that direction at low temperature. The blocking temperature T_b is identified with the temperature at which a maximum in the zero field cooled magnetization curve is observed. T_b can be associated with an average size of the particles. The point at which ZFC-FC starts to diverge is associated with the blocking temperature of the bigger particles.

The FC-ZFC curves at 500 Oe for cobalt ferrite nanoparticles are shown in Fig. 6. However, the blocking temperature of cobalt ferrite nanoparticles seems to be above room temperature. The relatively larger blocking temperature can be due to the large anisotropy contributions in cobalt ferrite nanoparticles. The TEM measurements reveal the nearly spherical nature of the cobalt ferrite nanoparticles. Hence, the contribution from surface and shape anisotropies cannot be expected in this case while the presence of uniaxial anisotropy is obvious from the squareness ratio. The shape of the FC branch is rather flat, showing a temperature independence which is a consequence of sizable interaction or aggregation effects resulting from dipolar interactions. Subsequently, the presence of uniaxial anisotropy and strong dipolar interactions directly influences the magnetic characteristics of cobalt ferrite.

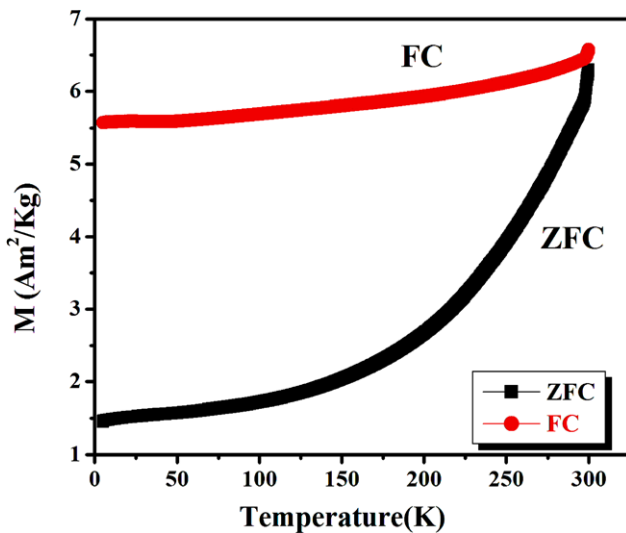


Fig. 6 FC-ZFC curves for CoFe_2O_4 (CP)

3.2 MCE measurements

For the estimation of the temperature range at which maximum cooling is produced, the $M-T$ curve of cobalt ferrite at 10 kOe is recorded and is shown in Fig. 7. A broad transition at around 150–350 K is clearly visible from the figure. This transition assumes significance in that an abrupt change in magnetization would normally be associated with a magnetic phase transition.

Further, the $M-H$ curves (Fig. 8) for cobalt ferrite nanoparticles over a magnetic field range of 0–13 kOe at 10 K temperature intervals from 173 to 323 K were measured. The MCE characteristic value (ΔS_m), i.e. the magnetic entropy change, was estimated from the $M-H$ curves using the relation in (3).

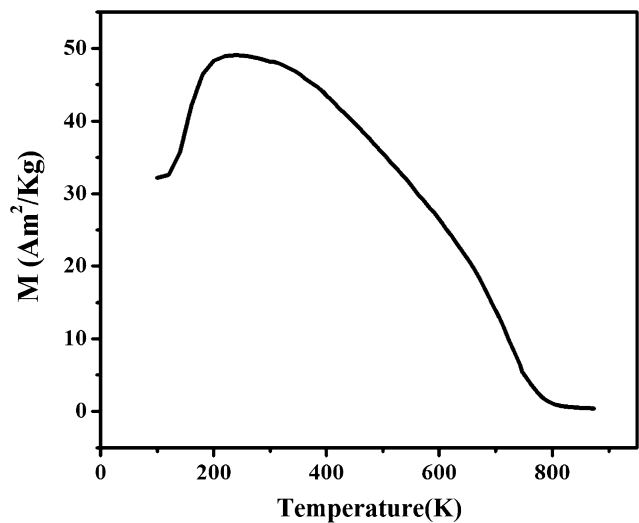


Fig. 7 $M-T$ curve at 10 kOe

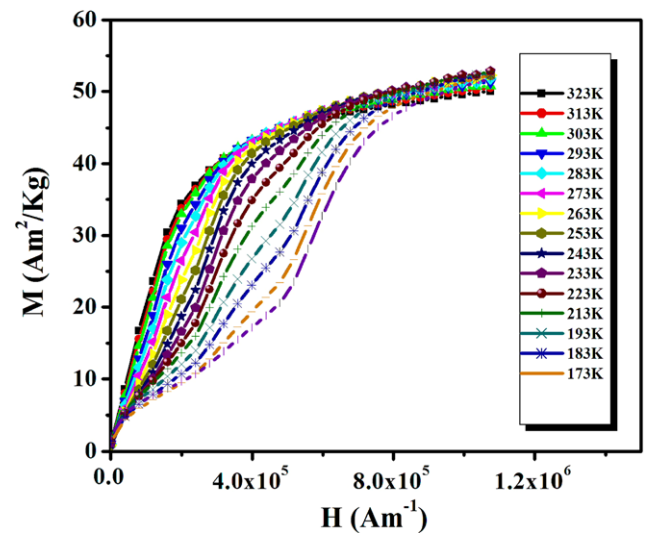


Fig. 8 Isothermal magnetization curves

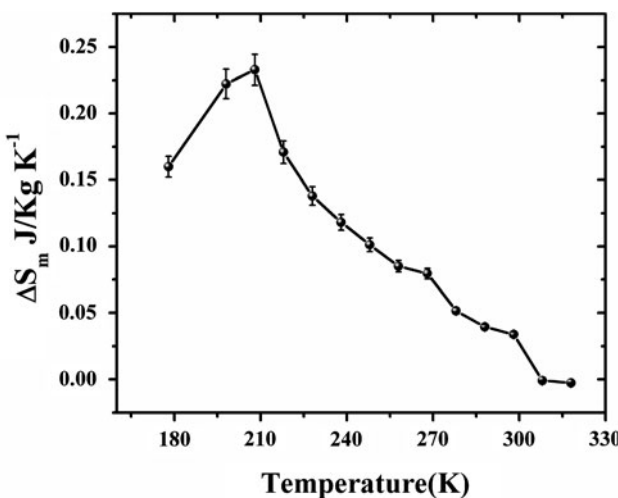


Fig. 9 Magnetic entropy change vs. temperature curve

Normally, we observe an increase in magnetization with decrease in temperature and expect a negative entropy change and accordingly term this a characteristic MCE. However, in this case, since there is a decrease in magnetization associated with the transition in this temperature range, the magnetic entropy change was found to be positive. Hence, this can be termed an inverse MCE. There are reports wherein giant inverse MCE has been observed in alloys like NiMnSb Heusler alloys [28, 29]. A positive entropy change has been recently reported in zinc ferrite nanoparticles [30].

The variation of magnetic entropy change with temperature is shown in Fig. 9. A maximum value of 0.23 J/kg K^{-1} is observed at 213 K for an applied field of 13 kOe. Thereafter, a sharp decrease is obtained. For 5-nm-sized cobalt ferrite nanoparticles prepared by the co-precipitation technique the maximum MCE value reported was 0.14 J/kg K^{-1} at an applied field of 35 kOe [10]. Hence, the magnitude of the maximum MCE value in our case is higher than that was reported for different ferrite nanoparticles like zinc ferrite, manganese zinc ferrite and nickel ferrite [9–12].

It may be noted that the ΔS_m value becomes negative at 308 K and is $-0.07 \text{ mJ/kg K}^{-1}$, which is also reasonable compared to MCE values reported in co-precipitated cobalt ferrite nanoparticles [10]. The change in the sign of ΔS_m around room temperature may be indicative of a blocking near this temperature for the nanoparticles. But, the blocking phenomenon, which is above 300 K, could not be observed from the FC–ZFC curves (Fig. 6) as they lie outside the measured temperature range. Hence, a detailed study is needed for tuning the material for room-temperature applications.

4 Conclusion

In conclusion, the magnetocaloric properties of cobalt ferrite nanoparticles, indirectly estimated from magnetization

isotherms, are presented here. The maximum calculated ΔS_m corresponding to an inverse MCE of $0.233 \text{ J/kg K}^{-1}$ was obtained at 213 K for an applied field of 13.5 kOe. The MCE value at this applied magnetic field of 13.5 kOe is relatively large when compared to the reported values. The inverse MCE value at around 308 K is suggestive of a transition in this region, which can be a blocking phenomenon occurring in these nanoparticles. The observation of inverse and large MCE values in cobalt ferrite nanoparticles proclaims the potential of cobalt ferrite for cooling and heating applications.

Acknowledgements EVG acknowledges Cochin University of Science and Technology (CUSAT) for a Research Fellowship and STIC, CUSAT for the ICP measurements. IAA would like to thank Sultan Qaboos University for support under Grant No. IG-SCI-PHYS-09-01. EVG gratefully acknowledges Dr. K.G. Suesh for the FC-ZFC measurements.

References

1. E. Warburg, Ann. Phys. **13**, 141 (1881)
2. W.F. Giaque, J. Am. Chem. Soc. **49**, 107B309864 (1927)
3. K.A. Gschneidner Jr., H. Takeya, J.O. Moorman, V.K. Pecharsky, S.K. Malik, C.B. Zimm, Adv. Cryog. Eng. **39**, 1457 (1997)
4. V.K. Pecharsky, K.A. Gschneidner Jr., Appl. Phys. Lett. **70**, 3299 (1997)
5. M.P. Annaorazov, M. Ünal, S.A. Nikitin, A.L. Tyurin, K.A. Asatryan, J. Magn. Magn. Mater. **251**, 61 (2002)
6. K.A. Gschneidner Jr., V.K. Pecharsky, C.B. Zimm, in *Proc. 50th Annu. Int. Appliance Technical Conf.*, West Lafayette, IN, 10–12 May 1999, p. 144
7. S.E. Lyshevski, *MEMS and NEMS: Systems, Devices, and Structures* (CRC Press, Boca Raton, 2002)
8. E. Brück, J. Phys. D, Appl. Phys. **38**, R381 (2005)
9. V.K. Pecharsky, K.A. Gschneidner Jr., Phys. Rev. Lett. **78**, 4494 (1997)
10. V.K. Pecharsky, K.A. Gschneidner Jr., Appl. Phys. Lett. **70**, 3299 (1997)
11. Z.B. Guo, W. Yang, Y.T. Shen, Y.W. Du, Appl. Phys. Lett. **70**, 904 (1997)
12. F.X. Hu, B.G. Shen, J.R. Sun, G.H. Wu, Phys. Rev. B **64**, 132412 (2001)
13. H. Wada, Y. Tanabe, Appl. Phys. Lett. **79**, 3302 (2001)
14. S. Hariharan, J. Gass, Rev. Adv. Mater. Sci. **10**, 398 (2005)
15. D. Peddis, C. Cannas, A. Musinu, G. Piccaluga, J. Phys. Chem. C **112**, 5141 (2008)
16. P. Poddar, J. Gass, D. Rebar, S. Srinath, H. Srikanth, S.A. Morrison, E.E. Carpenter, J. Magn. Magn. Mater. **307**, 227 (2006)
17. P. Jeppson, R. Sailer, E. Jarabek, J. Sandstrom, B. Anderson, M. Bremer, D.G. Grier, D.L. Schulz, A.N. Caruso, S.A. Payne, P. Eames, M. Tondra, J. Appl. Phys. **100**, 114324 (2006)
18. M. Veveřka, P. Veveřka, O. Kaman, A. Lančok, K. Závěta, E. Pollert, K. Knížek, J. Boháček, M. Beneš, P. Kašpar, E. Duguet, S. Vasseur, Nanotechnology **18**, 345704 (2007)
19. F. Figueiredo, A.C. Tedesco, P.C. Morais, J. Appl. Phys. **93**, 6707 (2003)
20. C. Vázquez-Vázquez, M. Lovelle, C. Mateo, M.A. López-Quintela, M.C. Buján-Núñez, D. Serantes, D. Baldomir, J. Rivas, Phys. Status Solidi A **205**, 1358 (2008)
21. A.H. Morrish, *The Physical Principles of Magnetism* (Wiley, New York, 1965), Chap. 3

22. K.A. Gschneidner Jr., V.K. Pecharsky, Mater. Sci. Eng. A **287**, 301 (2000)
23. K.A. Gschneidner Jr., V.K. Pecharsky, Annu. Rev. Mater. Sci. **30**, 387 (2000)
24. B. Vishwanathan, V.R.K. Moorthy, *Ferrite Materials: Science and Technology* (Springer, Berlin, 1960)
25. B.G. Toksha, S.E. Shrisath, S.M. Patange, K.M. Jadhav, Solid State Commun. **147**, 479 (2008)
26. C.N. Chinnasamy, B. Jeyadevan, K. Shinoda, K. Tohji, D.J. Djayaprawira, M. Takahashi, Appl. Phys. Lett. **83**, 2862 (2003)
27. E.C. Stoner, E.P. Wohlfarth, Philos. Trans. R. Soc. A **240**, 599 (1948)
28. T. Krenke, E. Duman, M. Acet, E.F. Wassermann, X. Moya, L. Mañosa, A. Planes, Nat. Mater. **4**, 450 (2005)
29. A.K. Nayak, K.G. Suresh, A.K. Nigam, J. Phys. D, Appl. Phys. **42**, 035009 (2009)
30. J. Gass, H. Srikanth, N. Kislov, S.S. Srinivasan, Y. Emirov, J. Appl. Phys. **103**, 07B309 (2008)